J|A|C|S ARTICLES

Published on Web 03/23/2009

Solution Structure and Thermodynamics of 2′,5′ RNA Intercalation

Eric D. Horowitz,[†] Seth Lilavivat,[†] Benjamin W. Holladay,[†] Markus W. Germann,[‡] and Nicholas V. Hud*,[†]

Parker H. Petit Institute of Bioengineering and Bioscience, Georgia Institute of Technology, School of Chemistry and Biochemistry, Atlanta, Georgia 30332-0400, and Georgia State University, Departments of Chemistry and Biology, Atlanta, Georgia 30302-4098

Received December 25, 2008; E-mail: hud@chemistry.gatech.edu

Abstract: As a means to explore the influence of the nucleic acid backbone on the intercalative binding of ligands to DNA and RNA, we have determined the solution structure of a proflavine-bound 2′,5′-linked octamer duplex with the sequence GCCGCGGC. This structure represents the first NMR structure of an intercalated RNA duplex, of either backbone structural isomer. By comparison with X-ray crystal structures, we have identified similarities and differences between intercalated 3′,5′ and 2′,5′-linked RNA duplexes. First, the two forms of RNA have different sugar pucker geometries at the intercalated nucleotide steps, yet have the same interphosphate distances. Second, as in intercalated 3′,5′ RNA, the phosphate backbone angle ζ at the 2′,5′ RNA intercalation site prefers to be in the *trans* conformation, whereas unintercalated 2′,5′ and 3′,5′ RNA prefer the *-gauche* conformation. These observations provide new insights regarding the transitions required for intercalation of a phosphodiester-ribose backbone and suggest a possible contribution of the backbone to the origin of the nearest-neighbor exclusion principle. Thermodynamic studies presented for intercalation of both structural RNA isomers also reveal a surprising sensitivity of intercalator binding enthalpy and entropy to the details of RNA backbone structure.

Introduction

A large number of planar, polycyclic heterocycles have been shown to intercalate the base pairs of DNA and RNA helices,[1] a mode of binding that can inhibit transcription,[2] replication,[3] and topoisomerase II activity *in vivo*.[4] Intercalation is one of the two most common modes of noncovalent drug−nucleic acid interaction, with the second being groove binding. Nevertheless, even after four decades of continuous study, our understanding of certain aspects of nucleic acid intercalation remains incomplete.[5] For example, the origin of the nearest-neighbor exclusion principle,[6] which states that intercalators can bind at no higher stoichiometry than one ligand per two base pairs, remains unresolved.[7] Even specific structural details associated with nucleic acid intercalation remain controversial, such as whether an alternating C3′ *endo*/C2′ *endo* sugar pucker along the nucleic acid backbone is a necessary condition for intercalative binding.[7a,8]

The energetics of intercalation are influenced by numerous elements of this coupled ligand binding-structural transition (e.g., electrostatics, dispersive interactions, solvent release, base pair destacking, restriction of conformational entropy).[9] One common and particularly dramatic feature of nucleic acid intercalation is the local unwinding of the double helix at the site of intercalation. It is therefore surprising that, despite numerous physical studies of DNA and RNA intercalation, there is a dearth of data relating to how backbone structure contributes to the thermodynamics and structural transitions associated with intercalation. It stands to reason that studying intercalation of non-natural backbones could provide fundamental new insights regarding the intercalation of natural nucleic acids.

2′,5′-Linked RNA is arguably the closest chemical analogue of native 3′,5′-linked RNA. However, the thermal stability and dynamics of duplexes formed by these two structural isomers are markedly different.[10] Thus, we hypothesized that duplex 2′,5′ RNA would respond differently to intercalation in comparison to natural RNA and, therefore, represents an excellent model system for probing the role of backbone structure in the thermodynamics and ligand specificity of nucleic acid intercalation.

[†] Georgia Institute of Technology.
[‡] Georgia State University.

(1) Leumann, C. J. *Bioorgan. Med. Chem.* **2002**, *10*, 841–854.
(2) Zunino, F.; Dimarco, A.; Zaccara, A.; Luoni, G. *Chem.-Biol. Interact.* **1974**, *9*, 25–36.
(3) Poot, M.; Hiller, K. H.; Heimpel, S.; Hoehn, H. *Exp. Cell Res.* **1995**, *218*, 326–330.
(4) Popanda, O.; Thielmann, H. W. *Carcinogenesis* **1992**, *13*, 2321–2328.
(5) (a) Lerman, L. S. *J. Mol. Biol.* **1961**, *3*, 18–30. (b) Ihmels, H.; Otto, D. *Top. Curr. Chem.* **2005**, *258*, 161–204.
(6) Crothers, D. M. *Biopolymers* **1968**, *6*, 575–584.
(7) (a) Voet, D. *Nature* **1977**, *269*, 285–286. (b) Friedman, R. A. G.; Manning, G. S. *Biopolymers* **1984**, *23*, 2671–2714. (c) Rao, S. N.; Kollman, P. A. *Proc. Natl. Acad. Sci. U.S.A.* **1987**, *84*, 5735–5739. (d) Williams, L. D.; Egli, M.; Gao, Q.; Rich, A. In *Structure and Function: Nucleic Acids*; Sarma, R. H., Sarma, M. H., Eds.; Adenine Press: Schenectady, NY, 1992; Vol. 1, pp 107−125.
(8) (a) Reddy, B. S.; Seshadri, T. P.; Sakore, T. D.; Sobell, H. M. *J. Mol. Biol.* **1979**, *135*, 787–812. (b) Berman, H. M.; Stallings, W.; Carrell, H. L.; Glusker, J. P.; Neidle, S.; Taylor, G.; Achari, A. *Biopolymers* **1979**, *18*, 2405–2429. (c) Shieh, H.-S.; Berman, H. M.; Dabrow, M.; Neidle, S. *Nucleic Acids Res.* **1980**, *8*, 85–97. (d) Dearing, A.; Weiner, P.; Kollman, P. A. *Nucleic Acids Res.* **1981**, *9*, 1483–1497. (e) Jain, S. C.; Sobell, H. M. *J. Biomol. Struct. Dyn.* **1984**, *1*, 1179–1194. (f) Aggarwal, A.; Islam, S. A.; Kuroda, R.; Neidle, S. *Biopolymers* **1984**, *23*, 1025–1041. (g) Neidle, S.; Abraham, Z. *CRC Cr. Rev. Biochem.* **1984**, *17*, 73–121.
(9) Chaires, J. B. *Biopolymers* **1997**, *44*, 201–215.

Previously, we demonstrated that a 2′,5′-linked RNA dodecamer exhibits an association constant, K_a, with proflavine that is 25-fold higher than that of a 3′,5′-linked RNA duplex with the same nucleotide sequence.[11] In contrast, the association constant of the 2′,5′ RNA duplex for ethidium is about half of that observed for the 3′,5′ RNA duplex.[11] The chemical moieties of ethidium and proflavine that intercalate Watson−Crick base pairs are somewhat similar. Both are comprised of three fused six-membered rings, both are positively charged at neutral pH, and both have exocyclic amino groups on either side of the long axis of their fused aromatic ring systems. A clear difference between these two intercalators is the presence of ethyl and phenyl pendant groups on ethidium, which are known to make van der Waals contacts in the minor groove of DNA.[8e] The observed difference in the relative affinity of these two molecules for 2′,5′ RNA, compared to both natural DNA and RNA, confirmed our hypothesis that the thermodynamics of intercalation is partly determined by backbone structure and also emphasized the significant role of the backbone in determining intercalator selectivity.

Although proflavine and ethidium are two well-studied RNA and DNA intercalators,[5a,12] our initial evidence that these molecules bind duplex 2′,5′ RNA (i.e., CD, UV−vis, fluorescence spectroscopy) was not sufficient to conclude that binding is through base pair intercalation. Proflavine, for instance, can also bind to the outside of duplex DNA, in addition to intercalative binding.[13] The NMR study presented here provides definitive proof that proflavine binds duplex 2′,5′ RNA through intercalation and suggests that particular backbone structural features are general to nucleic acid intercalation. A more thorough thermodynamic comparison of 2′,5′ and 3′,5′ RNA intercalation also shows the generality of a previously observed enthalpy−entropy relationship for intercalative binding. The potential importance of these results to resolving the elusive origin of the nearest neighbor exclusion principle is discussed.

Materials and Methods

Materials. 2′,5′ RNA was synthesized using standard phosphoramidite chemistry (ChemGenes). The full length dodecamer oligonucleotides were separated from failure sequences by denaturing PAGE, extracted from the gel by the crush-and-soak method, loaded onto a DEAE column (Whatman), washed with 150 mM NaCl, eluted with 2.5 M NaCl, ethanol precipitated, and desalted using a 1 m Sephadex G-10 column. 3′,5′ RNA oligos were purchased from Dharmacon Inc. and used without further purification.

Extinction coefficients for RNA oligonucleotides were determined by strand hydrolysis in 0.3 M NaOH[14] and comparison with reported nucleotide monophosphate extinction coefficients.[15] Extinction coefficients determined for 2′,5′ RNA were as follows: GCCGCGGC, 52 100 M^{-1} cm^{-1}; CCCGCCGCGCCG, 55 000 M^{-1} cm^{-1}; and CGGCGCGGCGGG, 71 600 M^{-1} cm^{-1}. For 3′,5′ RNA: CCCGCCGCGCCG, 52 100 M^{-1} cm^{-1} and CGGCGCGGCGGG, 71 100 M^{-1} cm^{-1}.

Ligand molecules, proflavine (Sigma-Aldrich), acridine orange (Sigma-Aldrich), and ethidium (Fisher Scientific) were purchased and used without further purification.

NMR Spectroscopy. For proflavine titrations and spectra with exchangeable proton resonances, NMR samples were 1 mM in 2′,5′ RNA duplex, 100 mM NaCl, 30 mM phosphate, pH 6.5, 10% D_2O. Spectra were collected at 275 K on a Bruker DRX500 Avance using the 3-9-19 WATERGATE pulse sequence.[16] Imino protons were assigned by 2D NOESY at 282 K. For spectra collected in D_2O, the final proflavine-titration sample was lyophilized and resuspended in 250 μL of 100% D_2O. 2D NOESY, ^{31}P-decoupled-COSY, ^{31}P−^{1}H HETCOR, and TOCSY spectra were collected on a Bruker 600 Avance at 282 K. NOESY spectra were acquired with mixing times of 75, 150, and 250 ms, which were confirmed to be within the linear range of the NOE growth. NOE peaks were separated into "strong", "medium", and "weak" intensities and were assigned ranges 1.8 to 2.7 Å, 1.8 to 3.3 Å, and 1.8 to 5.0 Å, respectively.

Structure Calculations. Molecular dynamics (MD) simulations were performed using AMBER 8.0,[17] with RNA described by the parm94 force field with the parmbs0[18] improvements. The 2′,5′ backbone was parametrized by exchanging the standard AMBER RNA charge and atom types for O3′ and H3′ with those of O2′ and H2′. The General AMBER Force Field[19] was used to parametrize proflavine. The Jaguar software package (Schrodinger) was used to calculate atomic charges using DFT with an HF/6−31G** basis set at the B3LYP level.

For the initial AMBER model, proflavine was manually docked into two intercalation sites that were introduced into an A-form 2′,5′ RNA duplex. Initial inspection of NOE constraints were consistent with proflavine being orientated in the same direction as had previously been observed in 3′,5′ RNA, i.e., with amino groups pointed toward the major groove.[8a,b] As a means to guard against modeling bias, an alternative model was also generated with proflavine rotated 180° with respect to the intercalated base pairs (i.e., with exocyclic amines facing the minor groove). Over the course of the simulated annealing, the NOE constraints caused the proflavine to reverse its orientation, thereby supporting our initial orientation of intercalated proflavine.

For annealing simulations, 4−10 ps of high temperature (400−4000 K) unrestrained MD was used to prepare 300 randomly generated starting structures, followed by a two-stage structure calculation process. During the first refinement, the molecule was heated to 800 K in the first 5 ps, cooled to 100 K for the next 13 ps, and then cooled to 0 K for the last 2 ps. The temperature of the system was maintained with a varying time constant: 0.4 ps during heating, 4 ps during cooling to 100 K, 1 ps for the final cooling stage, and then reduced from 0.1 to 0.05 for the last picosecond. The force constants for NOE constraints were increased from 3 to 30 kcal mol^{-1} $Å^{-2}$ during the first 5 ps and then maintained constant for the rest of the simulation. These force constants were applied in the form of a parabolic, flat-well energy term where r is the model distance or torsion angle and k is the respective force constant.

$$E_{\text{constraint}} = k(r_2 - r)^2 \qquad r_1 \le r < r_2$$
$$E_{\text{constraint}} = 0 \qquad r_2 \le r \le r_3$$
$$E_{\text{constraint}} = k(r_3 - r)^2 \qquad r_3 \le r < r_4$$

The values for r_1 and r_4 represent upper and lower distance bounds, defining the linear energetic penalty before and after the

(10) (a) Usher, D. A. *Nature-New Biol.* **1972**, *235*, 207–208. (b) Kierzek, R.; He, L. Y.; Turner, D. H. *Nucleic Acids Res.* **1992**, *20*, 1685–1690. (c) Giannaris, P. A.; Damha, M. J. *Nucleic Acids Res.* **1993**, *21*, 4742–4749. (d) Hannoush, R. N.; Damha, M. J. *J. Am. Chem. Soc.* **2001**, *123*, 12368–12374. (e) Plevnik, M.; Gdaniec, Z.; Plavec, J. *Nucleic Acids Res.* **2005**, *33*, 1749–1759.
(11) Horowitz, E. D.; Hud, N. V. *J. Am. Chem. Soc.* **2006**, *128*, 15380–15381.
(12) Waring, M. J. *J. Mol. Biol.* **1965**, *13*, 269–282.
(13) Schelhorn, T.; Kretz, S.; Zimmermann, H. W. *Cell. Mol. Biol.* **1992**, *38*, 345–365.
(14) Cohn, W. E. *Methods Enzymol.* **1957**, *3*, 724–743.
(15) Cavaluzzi, M. J.; Borer, P. N. *Nucleic Acids Res.* **2004**, *32*, e13.
(16) Piotto, M.; Saudek, V.; Sklenar, V. *J. Biomol. NMR* **1992**, *2*, 661–665.
(17) Pearlman, D. A.; Case, D. A.; Caldwell, J. W.; Ross, W. S.; Cheatham, T. E.; Debolt, S.; Ferguson, D.; Seibel, G.; Kollman, P. *Comput. Phys. Commun.* **1995**, *91*, 1–41.
(18) Perez, A.; Marchan, I.; Svozil, D.; Sponer, J.; Cheatham, T. E.; Laughton, C. A.; Orozco, M. *Biophys. J.* **2007**, *92*, 3817–3829.
(19) Wang, J. M.; Wolf, R. M.; Caldwell, J. W.; Kollman, P. A.; Case, D. A. *J. Comput. Chem.* **2004**, *25*, 1157–1174.

flat-well energy term. Distance constraints between base pairs, set at half the NOE distance constraint strength, were applied to maintain hydrogen bonding (as indicated by the observation of imino proton resonances). Planarity force constraints of 25 kcal mol^{-1} rad^{-2} were applied to the proflavine molecules throughout the simulations. Planarity force constraints of 200 kcal mol^{-1} rad^{-2}, on N9 of purines and N1 of pyrimidines, were used to maintain the glycosidic bond in plane with the bases. Backbone constraints, including ribose pseudorotation, α and ζ torsion angles, were held with force constants of 1000 kcal mol^{-1} rad^{-2} based on ^{31}P chemical shift analysis.[20] The backbone angles β ($P_{(i-1)}-O5'_{(i)}-C5'_{(i)}-C4'_{(i)}$), γ (O5′−C5′−C4′−C3′), and ϵ (C3′−C2′−O2′−P) were not constrained because of insufficient $^{1}H-^{1}H$ and $^{31}P-^{1}H$ coupling data, which would define these angles.

The 30 lowest energy structures were each subjected to a second stage of restrained molecular dynamics using the Generalized Born implicit solvent model.[21] The temperature profile, simulation length, constraint forces were identical to those of the first refinement procedure. Ten structures with the lowest energy and NOE violations were selected for the final ensemble and analyzed using VMD.[22] The helical parameters for the 10 lowest energy structures were analyzed using CURVES.

Fluorescence Spectroscopy. Fluorescence measurements were performed on a Shimadzu RF-5301PC spectrofluorophotometer at 298 K. Sample buffer was 1 × BPE (8 mM sodium phosphate, 1 mM Na_2EDTA, pH 7) and 100 mM NaCl. Small volumes (e.g., 1 μL) of a concentrated stock of nucleic acid that also contained 1 μM ligand were added to a 200 μL 1 μM solution of ligand. Excitation and emission wavelengths and bandwidths were as follows: proflavine, 455 nm, 1.5 nm, 5 nm; acridine orange, 475 nm, 1.5 nm, 5 nm; ethidium, 510 nm, 5 nm, 10 nm. Equilibrium constants were derived as described by Qu and Chaires.[23] All titrations were performed in triplicate.

Isothermal Titration Calorimetry. ITC measurements were performed using a Microcal VP-ITC at 298 K. For model-free determination of ligand binding enthalpy,[24] each injection was 5 μL of 125 μM ligand with the sample cell initially containing 1.4 mL of 250 μM nucleic acid (in bp). Final enthalpy values were determined by fitting a Gaussian curve to histograms of evolved heat per mole of ligand (corrected for heat of dilution) from multiple injections (Supporting Information). Sample buffer was 100 mM NaCl, 1 × BPE, pH 7.

Results

^{1}H NMR confirms proflavine intercalation of 2′,5′ RNA. Titration of the 2′,5′ RNA duplex $(GCCGCGGC)_2$ with proflavine to a stoichiometry of two proflavine molecules per duplex was monitored by ^{1}H NMR spectroscopy (Figure 1). Over the course of titration, the three original imino resonances disappeared, and four new imino resonances were observed at a proflavine/duplex concentration of 2:1. Additionally, an intermediate set of resonances was observed between these initial and final stages of the titration (Figure 1). The coexistence of these intermediate resonances with the initial and final resonances reveals that duplexes with different levels of proflavine loading are in slow exchange on the NMR time scale.

While the ^{1}H NMR spectrum of the ligand-free duplex contains only three imino resonances, more than four imino

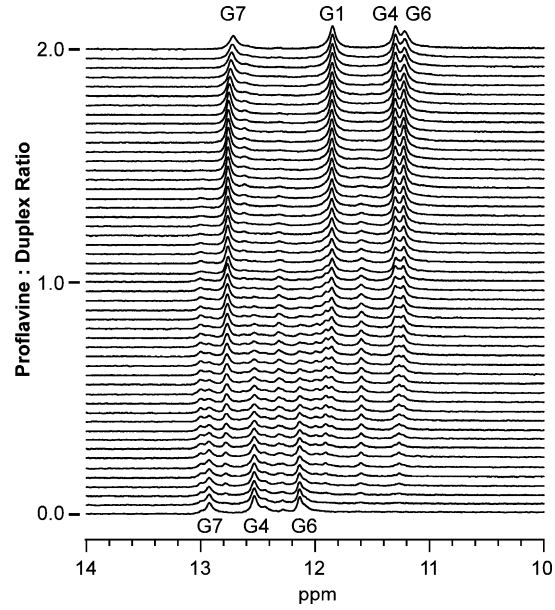

Figure 1. ^{1}H NMR of the imino proton region over the course of proflavine titration into a 2′,5′ RNA duplex $(GCCGCGGC)_2$ at 275 K. Duplex concentration was 1 mM; proflavine concentrations ranged from 0 to 2 mM. Each proflavine addition was in increments of 0.04 mol equiv to RNA duplex. Proton assignments for the proflavine-free sample (bottom) are from the work of Premraj et al.[25] Proton assignments for the top spectrum are based upon 2D NOESY assignments.

resonances are associated with the intermediate stages of the titration (most apparent for proflavine:duplex ratios of 0.5:1 and 1:1). This greater number of resonances is consistent with a break in the symmetry of the RNA duplex upon the binding of a single proflavine molecule. The symmetry of the proflavine-bound duplex is recovered at the last stage, where two proflavine molecules must be bound at two symmetry-related sites.

The four imino protons in the final proflavine titration sample (2:1 proflavine/duplex) were assigned by 2D ^{1}H NMR. These resonances are shifted upfield from the corresponding imino proton resonances of the unbound (proflavine-free) duplex. An upfield shift in imino proton resonance has been shown to correlate with binding by intercalation, rather than groove binding or outside stacking along the phosphate backbone.[26]

The appearance of a fourth imino proton resonance from the terminal base pairs illustrates that this proton is in slow exchange with solvent protons in the proflavine-bound duplex. This reduced rate of exchange could be due to a reduced fraying of the duplex ends due to proflavine stabilization of the duplex[11] or increased end-to-end stacking of proflavine-bound duplexes, which would also protect the terminal imino protons from solvent exchange.[27] Evidence for end-to-end stacking for the proflavine-bound duplex was observed in the form of weak NOEs between G1 and C8 (data not shown).

Solution Structure of Proflavine-Bound 2′,5′ RNA. The aromatic-H1′ region of a 2D ^{1}H NOESY spectrum, with the intra- and inter-residue aromatic-H1′ NOE "walk-through,"[28] is shown in Figure 2 for the 2′,5′ RNA duplex with bound proflavine. The G1H8−G1H1′ cross peak exhibits a greater intensity than other comparable NOEs (e.g., compared to

(20) Mazzini, S.; Mondelli, R.; Ragg, E. *J. Chem. Soc., Perkin Trans. 2* **1998**, 1983–1991.
(21) Tsui, V.; Case, D. A. *J. Am. Chem. Soc.* **2000**, *122*, 2489–2498.
(22) Humphrey, W.; Dalke, A.; Schulten, K. *J. Mol. Graphics* **1996**, *14*, 33–38.
(23) Qu, X. G.; Chaires, J. B. *Methods Enzymol.* **2000**, *321*, 353–369.
(24) Haq, I.; Jenkins, T. C.; Chowdhry, B. Z.; Ren, J. S.; Chaires, J. B. *Methods Enzymol.* **2000**, *323*, 373–405.
(25) Premraj, B. J.; Patel, P. K.; Kandimalla, E. R.; Agrawal, S.; Hosur, R. V.; Yathindra, N. *Biochem. Biophys. Res. Commun.* **2001**, *283*, 537–543.
(26) Feigon, J.; Denny, W. A.; Leupin, W.; Kearns, D. R. *J. Med. Chem.* **1984**, *27*, 450–465.
(27) Reinhardt, C. G.; Krugh, T. R. *Biochemistry* **1978**, *17*, 4845–4854.
(28) Wüthrich, K. *NMR of Proteins and Nucleic Acids*; John Wiley & Sons, Inc.: New York, NY, 1986.

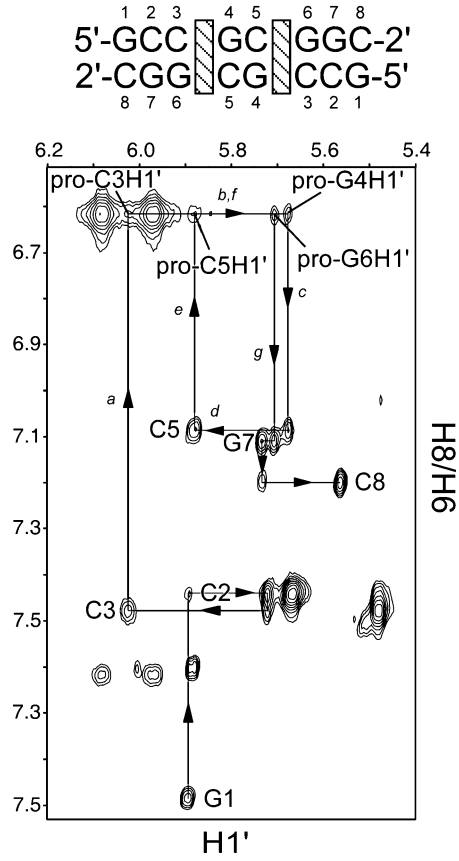

Figure 2. Aromatic-H1′ region of a 2D NOESY of the 2′,5′ RNA duplex $(GCCGCGGC)_2$ with bound proflavine. The aromatic-H1′ NOE walk-through along the duplex is shown. At the intercalation site, the proflavine resonance H2/H7 is used in lieu of the adjacent base. Arrows marked *a* through *g* guide through the proflavine-RNA NOE connectivity. RNA concentration was 2 mM in duplex, and proflavine was 4 mM. The spectrum was acquired with a mixing time of 250 ms at 600 MHz in D_2O, 282 K, 60 mM phosphate buffer pH 6.5, 200 mM NaCl.

G1H8−G1H2′). A similar observation has previously been reported for the 5′-terminal nucleotide of 2′,5′ RNA and 2′,5′ DNA duplexes and has been attributed to the glycosidic bond being in the *syn* conformation.[10e,25,29]

Intercalation can cause the local unwinding of a base step such that the H1′ proton of the 5′-nucleotide and the aromatic proton of the 3′-nucleotide that flank the intercalation site are separated beyond the limit of the nuclear Overhauser effect (i.e., >6 Å).[30] Accordingly, the cross peaks that would correspond to the C3H1′−G4H8 and C5H1′−G6H8 NOEs of a standard duplex are not observed (Figure 2). However, the NOE walk-through can be continued through a proflavine resonance assigned to the chemically equivalent H2 and H7 protons. These NOE cross peaks also confirm the binding site of proflavine to the two symmetry-related 5′-CpG-2′ dinucleotide steps (C3pG4 and C5pG6). Interestingly, the same preference for CpG steps over CpC, GpC, and GpG steps has long been appreciated for 3′,5′ DNA and RNA duplexes.[8a,b,e,f,31]

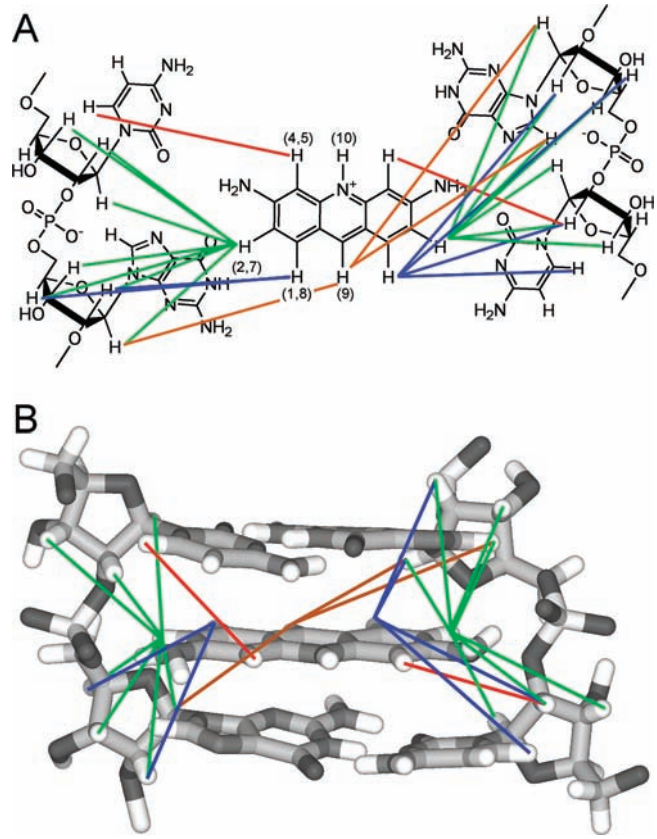

Figure 3. (A) Diagram illustrating the NOEs observed between proflavine and the CpG steps of the 2′,5′ RNA duplex. The IUPAC acridine numbering is shown around the proflavine ring. (B) Diagram illustrating the 3D spatial arrangement of the NOEs shown in image A (viewed from the major groove). Structure shown is the lowest energy NMR-derived structure.

RNA and proflavine proton assignments were made based on 2D COSY, TOCSY, and NOESY (Supporting Information). Twenty-five NOEs were observed between proflavine and the RNA duplex, which define the position of proflavine within the CpG binding site (Figure 3). In the lowest energy calculated structures, proflavine is aligned such that the exocyclic amines face the major groove, similar to the orientation of proflavine in the cocrystal with the 3′,5′ CpG dinucleotide.[8a,b,f]

$^{31}P-^{1}H$ HETCOR heteronuclear spectroscopy was used to assign the seven phosphorus resonances of the 2′,5′ RNA duplex, with and without 2 molar equiv of proflavine. The two ^{31}P resonances associated with the intercalation sites (C3pG4 and C5pG6) are shifted downfield from the unintercalated phosphorus resonances by *ca.* 1 ppm (Figure 4). This downfield shift is consistent with what has been previously observed for a BI to BII transition in the DNA backbone[32] and is also associated with intercalation of DNA.[33] The backbone torsion angles ζ and α, corresponding to $C2'_{(i)}-O2'_{(i)}-P_{(i)}-O5'_{(i+1)}$ and $O2'_{(i)}-P_{(i)}-O5'_{(i+1)}-C5'_{(i+1)}$, respectively, influence ^{31}P chemical shift, and correlations have been made between ζ and α angles and ^{31}P chemical shift.[34] Based upon these previous correlations, the downfield shifts of the phosphorus nuclei at the intercalation site correspond to ζ and α angles of 180 ± 60° (*trans*) and −60 ± 60° (*-gauche*), respectively, whereas the phosphorus

(29) (a) Robinson, H.; Jung, K. E.; Switzer, C.; Wang, A. H. J. *J. Am. Chem. Soc.* **1995**, *117*, 837–838. (b) Premraj, B. J.; Raja, S.; Bhavesh, N. S.; Shi, K.; Hosur, R. V.; Sundaralingam, M.; Yathindra, N. *Eur. J. Biochem.* **2004**, *271*, 2956–2966.
(30) (a) Gilbert, D. E.; Feigon, J. *Biochemistry* **1991**, *30*, 2483–2494. (b) Spielmann, H. P.; Wemmer, D. E.; Jacobsen, J. P. *Biochemistry* **1995**, *34*, 8542–8553.
(31) Adams, A. *Curr. Med. Chem.* **2002**, *9*, 1667–1675.
(32) Gorenstein, D. G. *Methods Enzymol.* **1992**, *211*, 254–286.
(33) Williams, H. E. L.; Searle, M. S. *J. Mol. Biol.* **1999**, *290*, 699–716.
(34) Gorenstein, D. G., Goldfield, E. M. *Phosphorous-31 NMR: Principles and Applications*; Academic Press: 1984; pp 299−316.

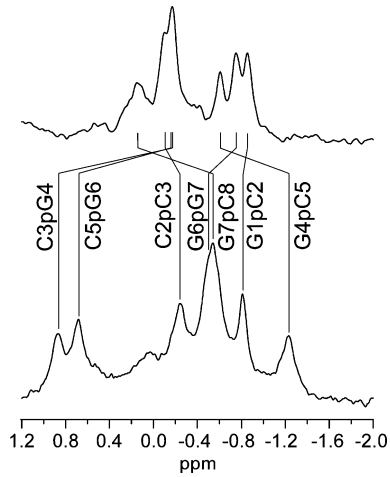

Figure 4. ^{1}H-decoupled ^{31}P NMR spectra of the 2′,5′ RNA duplex $(GCCGCGGC)_2$ at 242.9 MHz. Spectra shown are of the unintercalated duplex (Top) and the intercalated duplex containing two proflavine molecules per duplex (Bottom). Spectra were collected at 282 K and processed with 6 Hz line broadening. See Materials and Methods for more experimental details.

Table 1. Three Bond Coupling Constants for the H1′−H2′ Correlations

	^{3}J H1′−H2′ (Hz)	sugar pucker
G1	7	C2′ *endo*
C2	<1.5[a]	C3′ *endo*
C3	8	C2′ *endo*
G4	<1.5[a]	C3′ *endo*
C5	6	C2′ *endo*
G6	<1.5[a]	C3′ *endo*
G7	5	C2′ *endo*/C3′ *endo*
C8	5	C2′ *endo*/C3′ *endo*

[a] Values could not be determined experimentally; the upper limit of 1.5 Hz coupling is based on resonance line width and resolution limits of 2D spectra.

nuclei at the unintercalated sites have chemical shifts that correspond to ζ and α angles of −60 ± 60° (*-gauche*) and −60 ± 60° (*-gauche*).

Correlations and three-bond coupling constants between H1′ and H2′ resonances, observed using the phase-sensitive ^{31}P-decoupled COSY experiment, were used to determine ribose sugar conformations (Table 1). The ribose coupling constants of residues G1, C3, and C5 are consistent with a *South* sugar pucker conformation (i.e., C2′ *endo*), while those of G7 and C8 are consistent with a mixed state between *South* and *North* conformations. H1′−H2′ COSY crosspeaks were not observed for residues C2, G4, and G6. An absence of H1′−H2′ crosspeaks could be caused by small coupling constants, which in conjunction with broad line shapes decreases the intensity of the crosspeak. Therefore, a lack of a crosspeak is indicative of a *North* conformation (i.e., C3′ *endo*).[35] Thus, at the intercalated 5′-CpG-2′ steps sugar conformations were *South* for the 5′ residues (i.e., C3 and C5) and *North* for the 2′ residues (i.e., G4 and G6). *This arrangement of sugar puckers around the intercalation site is the converse of that observed in 3′,5′ linked DNA and RNA duplexes*, in which the sugar of the 5′ pyrimidine residue of an intercalation site is typically in a *North* conformation and the sugar of the 3′ purine residue is in the *South* conformation.[36]

Table 2. Structural Statistics for the 10 Lowest Energy Structures[a]

NOE-derived distance constraints	189
intranucleotide NOEs	119
internucleotide NOEs	70
pseudorotation angle constraints	8
backbone torsion angle constraints	14
H-bond constraints	40
NOE violations > 1.0 Å	0
NOE violations > 0.5 Å	4.4[b]
rmsd	0.80 Å

[a] The numbers for non-H-bond constraints shown represent the constraints from only one strand. [b] The number of violations >0.5 Å were between 3 and 5 for the 10 lowest energy structures.

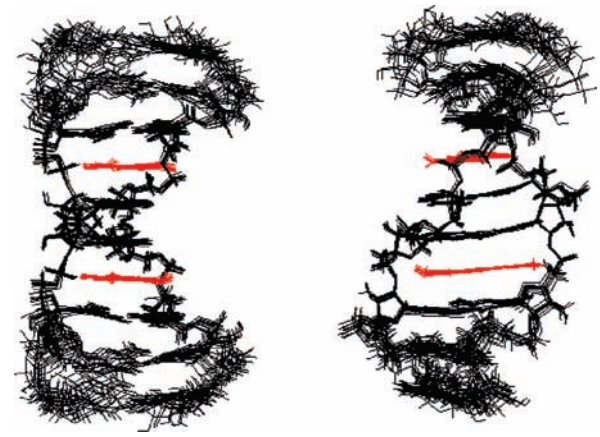

Figure 5. Superimposition of the 10 lowest-energy NMR-derived structures for the 2′,5′ RNA duplex $(GCCGCGGC)_2$ with bound proflavine. The structures are superimposed with respect to the two proflavine molecules (shown in red). Structures are shown from the side (Left) and from the minor groove (Right) of the central base step. The lowest energy structure is deposited in the PDB (ID *2KD4*).

The number of G1−C2 and G7−C8 inter-residue NOEs were about twice the number observed for the other nucleotide steps, and as mentioned above, mixed sugar pucker conformations were observed for G7 and C8. When all constraints for these two terminal nucleotide steps were applied during structure refinement, the terminal base C8 appeared to be held rigidly and in an orientation that was atypical of a terminal duplex nucleotide base. We hypothesized that the unusually large number of constraints, and two sugar conformations, were indicative of the terminal base pairs existing in two different conformations, corresponding to the *anti* and *syn* glycosidic bonds of G1. In order to not distort the helix beyond the first base pair by the simultaneous application of apparently incompatible constraints, the structure was calculated using only the observed G1/C8−C2/G7 internucleotide constraints that were consistent with the *syn* glycosidic bond of G1. Thus, the structure of the terminal base pairs only represents one of two conformations that appear to coexist in equilibrium.

The constraints shown in Table 2 were used with the AMBER suite of programs to refine a solution state model of the intercalated 2′,5′ RNA duplex (Materials and Methods). The 10 lowest energy structures converged with an all atom rmsd of 0.80 Å (Figure 5). When these structures are aligned relative to the proflavine molecules, the base pairs surrounding the intercalation sites are very well-defined (Figure 5).

(35) Evans, J. N. S. *Biomolecular NMR Spectroscopy*; Oxford University Press: New York, NY, 1995.

(36) Patel, D. J.; Shen, C. *Proc. Natl. Acad. Sci. U.S.A.* **1978**, *75*, 2553–2557.

This structure of a proflavine-intercalated 2′,5′ RNA duplex has a helical twist of only 22° at the CpG steps, while the base steps flanking the intercalation sites have helical twists of 42°, 49°, and 42° (C2pC3, G4pC5, and G6pG7, respectively) (Supporting Information). These helical twist values at unintercalated steps are consistent with those previously observed for the same (unintercalated) 2′,5′ RNA duplex.[25] The 2′,5′ RNA double helix therefore unwinds by an average of 22° at each intercalation site, which is somewhat larger than the unwinding angle observed for proflavine-bound 3′,5′ nucleic acids (i.e., *ca.* 17°).[8g] This difference could be the result of 3′,5′ RNA having a lower unintercalated helical twist (33°) than 2′,5′ RNA,[37] and that the twists of intercalated steps are similar for both forms of RNA.

The helical rise of the base steps neighboring the intercalation sites is larger than that which was observed for the native duplex (*ca.* 3.8 vs 2.5 Å[25]) (Supporting Information). This observation arises from the unwound intercalation sites causing the neighboring base pairs to be perpendicular to the helical axis. Our NMR model shows that the native helical rise of 2.5 Å increases to 6.6 Å upon intercalation. The increased helical rise at the intercalated base steps is similar to that which is observed for 3′,5′ RNA upon intercalation (i.e., from *ca.* 2.9 to 6.8 Å).[5a,8b,37] The negative slide values of the unintercalated base steps are consistent with an A-form helix and are very similar to what was previously reported for unintercalated 2′,5′ RNA.[25]

Backbone Conformational Analysis. As mentioned above, a downfield change in ^{31}P chemical shift had previously been correlated with a change in the backbone angle ζ from −60° (*-gauche*) to 180° (*trans*) while α remains constant at −60° (a BI to BII conformational transition), but for native 3′,5′-linked RNA. To test if our observed changes in ^{31}P chemical shift for 2′,5′ RNA were also indicative of a change in the ζ angle, the constraints that had been applied to the backbone angles were removed and the simulated annealing protocol was repeated. Analysis of the resulting ζ angle conformations revealed a very similar grouping of angles as that which resulted from structures refined with the ^{31}P chemical shift-derived ζ angle constraints (i.e., *-gauche*/*trans* for unintercalated and intercalated phosphates, respectively) (Supporting Information). Thus, the distance constraints and sugar pucker constraints derived from the NMR data are consistent with the correlation between changes in ^{31}P chemical shift and ζ angle as determined previously for 3′,5′ DNA and RNA. Additionally, when torsional constraints opposite to those derived from ^{31}P chemical shift changes were used (unintercalated phosphates with ζ angles of 180° and intercalated phosphates with ζ angles of −60°), the ζ angles after simulated annealing exhibit a peculiar distribution. First, a narrow distribution of angles was observed near the edge of the window of angles allowed by the applied constraints, implying that the most favorable conformation (as defined by the NMR constraints and the AMBER force field) is beyond the defined ζ angle allowed range (±60°). Second, the resulting rmsd was higher between the lowest energy structures (1.41 Å). These observations strongly support the ^{31}P chemical shift correlations derived for the ζ angles of 3′,5′ DNA and RNA as being applicable to defining the backbone of 2′,5′ RNA.[10e]

To test if sugar pucker and ζ phosphate angles are necessarily correlated at a site of intercalation in 2′,5′ RNA, simulated annealing was carried out with distance constraints held constant, but with the ζ angle constraints removed and sugar pucker constraints flipped (C3′ *endo* to C2′ *endo*, and visa versa). The resulting ζ angles did not converge to Gaussian distributions as they did when the experimentally derived sugar pucker constraints were used. These structures also had a higher rmsd (0.99 Å) and more NOE violations greater than 2 Å as compared to no violations greater than 2 Å with the experimentally determined sugar pucker constraints (Table 2). This result supports the existence of a structural correlation between sugar pucker and ζ angle at the site of intercalation, implying that C2′ *endo*/C3′ *endo* sugar puckers and a trans (180°) ζ angle are also characteristic of an unwound 2′,5′ RNA helix at the site of intercalation.

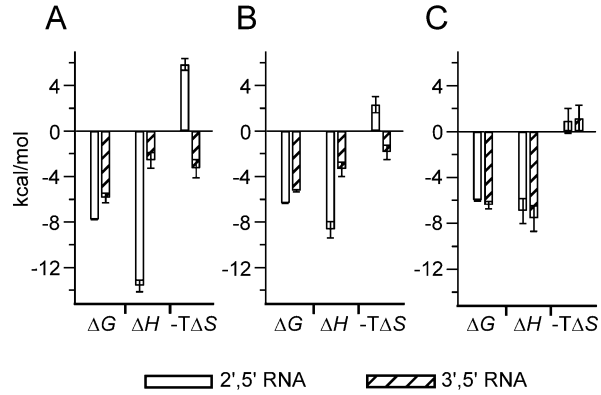

Figure 6. Thermodynamic values for the binding of three known intercalators to 2′,5′ RNA and 3′,5′ RNA at 25 °C. (A) proflavine, (B) acridine orange, and (C) ethidium. Error bars represent standard deviations. Enthalpy values were determined by ITC. Free energy values were determined by both ITC and fluorescence-monitored titration. For more information see Materials and Methods. Thermodynamic values are provided in tabular format in the Supporting Information.

Thermodynamics of 2′,5′ RNA Intercalation. Previously, we reported that the association constant of proflavine for duplex 2′,5′ RNA was 25-fold greater compared to duplex 3′,5′ RNA.[11] The fact that 2′,5′ RNA binds proflavine more favorably than 3′,5′ RNA, whereas ethidium was found to bind *less* favorably, indicated that one of these two forms of RNA does not simply bind all intercalators more favorably than the other. To better characterize this difference in binding thermodynamics, we have determined the enthalpy and entropy of proflavine, ethidium, and acridine orange binding to 2′,5′ RNA and 3′,5′ RNA (Figure 6).

Using isothermal titration calorimetry (ITC) it was determined that proflavine binds 3′,5′ RNA with a ΔH of −2.6 kcal/mol and 2′,5′ RNA with a ΔH of −13.6 kcal/mol, for a remarkable difference of −11.0 kcal/mol. Given that the ΔG of proflavine binding to 2′,5′ RNA is −7.8 kcal/mol at 25 °C, the entropy of binding, calculated as $-T\Delta S = \Delta G - \Delta H$, is +5.8 kcal/mol. In contrast, the ΔG of proflavine binding to 3′,5′ RNA is −5.9 kcal/mol at 25 °C, which implies that $-T\Delta S$ is −3.3 kcal/mol. Thus, although the ΔG of proflavine binding to the two forms of RNA differs by only *ca.* 2 kcal/mol, proflavine binding to 3′,5′ RNA is entropically favored, whereas proflavine binding to 2′,5′ RNA is *not* entropically favored (Figure 6).

Acridine orange, which is structurally similar to proflavine, was also determined to have a favorable ΔH of −8.7 kcal/mol and unfavorable $-T\Delta S$ of +2.3 kcal/mol for binding to 2′,5′ RNA. The difference in acridine orange binding to 3′,5′ RNA follows that same trend as proflavine (i.e., more favorable

(37) Bloomfield, V. A.; Crothers, D. M.; Tinoco, I. *Nucleic Acids: structures, properties, and functions*; University Science Books: Sausalito, CA, 2000.

enthalpy and less favorable entropy for 2′,5′ RNA), but the difference in these thermodynamic parameters is not as great as that observed for proflavine (Figure 6). In contrast to proflavine and acridine orange, the enthalpy and entropy of ethidium binding do not vary appreciably between the two RNA structural isomers. For these three intercalators, a plot of entropy versus enthalpy of binding, as described by Chaires for small molecule DNA ligands,[38] reveals a trend in enthalpy−entropy compensation that appears to be universal for simple intercalators. While the source of this apparent enthalpy−entropy compensation for DNA binding is not revealed by such analysis, it nevertheless appears that this trend is likewise followed by the thermodynamics of 2′,5′ RNA intercalation (Supporting Information).

Discussion

Structural Features of 2′,5′ RNA Intercalation. For 3′,5′ RNA and DNA duplexes intercalation is most favored at Py-p-Pu steps.[7a] This preference has been attributed to the relatively poor intrastrand base stacking at Py-p-Pu steps,[39] which makes base *destacking* upon intercalation *less unfavorable* than at other steps. The structure reported here of proflavine-intercalated 2′,5′ RNA provides direct evidence that, for the sequence studied, Py-p-Pu steps are also preferred sites of intercalation. It has been suggested that all intrastrand base stacking within a 2′,5′ RNA duplex is less favorable than that in a 3′,5′ RNA duplex.[10b,40] It was therefore not obvious at the start of this investigation whether the CpG step would be the most favored site for intercalation by proflavine.

Inter- and Intramolecular Hydrogen Bonding in the Proflavine-2′,5′ RNA Complex. The proflavine−2′,5′ RNA structure reported here revealed optimal H-bonds between the amino groups of proflavine and phosphate oxygens (H−O distances of *ca.* 1.9 Å). These interactions likely contribute to the comparatively high association constant between proflavine and 2′,5′ RNA (further discussed below). In addition, H-bonds between the 3′-OH and phosphate oxygen atoms exist at every base step. This structural feature was also noted by Premraj et al.,[25] and we have found that this intriguing intrabackbone H-bonding of a 2′,5′ RNA duplex is maintained even at intercalated steps.

2′,5′ RNA Intercalation Structural Requirements. Voet proposed that the apparent necessity for alternating sugar puckers in an intercalated duplex could provide an energetic barrier that restricts intercalation to one ligand binding between every other base pair (i.e., the nearest-neighbor exclusion principle).[7a] However, intercalated duplexes without alternating sugar puckers have been observed, with these exceptions being attributed to H-bonding between the intercalating molecule and the phosphate backbone.[8b,f] Based upon computational studies, Kollman and co-workers argued that the alternating C3′ *endo*/C2′ *endo* (*North*/*South*) sugar pucker conformations around an intercalation site is energetically more favorable but likewise concurred that ligand interactions with the phosphate backbone could cause intercalation sites with nonalternating sugar puckers to exist.[8d] Although more recent calculations regarding the nearest-neighbor exclusion principle and intercalation energetics have been conducted with more current force-field parameters,[7c,41] the energetics of alternating sugar puckers at intercalation sites has apparently not since been reinvestigated.

The sugar puckers around a 2′,5′ RNA intercalation site was found here to alternate between *South* and *North* conformations for the pyrimidine and purine bases, respectively, which is exactly the opposite of the trend discussed above for natural RNA. This difference seems to be very large at first glance. However, it was noted by Premraj et al. that, while (unintercalated) 2′,5′ RNA and 3′,5′ RNA helices have different sugar puckers (C2′ *endo* and C3′ *endo,* respectively), the two forms of RNA maintain a similar phosphate−phosphate distance of 5.9 Å. These authors termed this state of the RNA backbone the *compact form.*[29b,40] The sugar pucker associated with the compact form is in contrast to the *extended form* sugar pucker (C3′ *endo* for 2′,5′ RNA and C2′ *endo* for 3′,5′ RNA), which places the phosphate−phosphate distance at 7−7.5 Å.[10e,42] Using this terminology, the sugar pucker geometries at the intercalation site in 2′,5′ RNA are compact/extended (Py/Pu) and are therefore actually the same, or at least analogous, to that which has been observed for 3′,5′ RNA, which is also compact/extended (Py/Pu) at an intercalation site.

When the opposite arrangement of sugar puckers was forced on the intercalation site, during structure refinement, the angle ζ was found to rotate into unfavorable conformations that were less well-defined, thereby increasing the rmsd of the lowest energy structures and the number of NOE constraint violations. This observation indicates that the extended conformation of the purine nucleoside and the change in the phosphate angle ζ allow for the formation of an intercalation site, and therefore these structural features are required for proflavine-2′,5′ RNA intercalation. In addition, intercalation at the CpG steps is consistent with the recent observation that CpG steps prefer the unwound BII conformation (trans ζ) in DNA.[43] The common observation of the compact/extended sugar pucker conformations, as well as the *trans* ζ angle conformation, in intercalated 3′,5′ DNA and RNA lends support to the proposal that these features are general structural requirements for intercalation of a nucleic acid with a phosphate-ribose backbone. Exceptions to this case may include intercalators that bind in perpendicular orientations to the base pairs, such as daunomycin, in which case there is significant base pair buckling and less duplex unwinding.[7d] Additionally, the extensive backbone interactions of molecules like daunomycin to 3′,5′ nucleic acids may stabilize the homogeneous compact/compact sugar pucker conformation.[8b,f]

2′,5′ RNA Intercalation Thermodynamics. It was surprising to observe such a large difference between the thermodynamics of proflavine binding to 2′,5′ RNA versus 3′,5′ RNA, especially given that no appreciable difference was observed for ethidium binding. Hydrogen bonding by the exocyclic amines of proflavine to phosphate oxygens could be a source of significant binding enthalpy in the 2′,5′ RNA complex. The positive charge of proflavine, often drawn only on the protonated N10 nitrogen, is likely delocalized such that partial positive charge resides on the exocyclic amino groups. The resulting charge−charge interactions between these amino groups and the anionic

(38) Chaires, J. B. *Arch. Biochem. Biophys.* **2006**, *453*, 26–31.
(39) Broyde, S.; Hingerty, B. *Biopolymers* **1979**, *18*, 2905–2910.
(40) Premraj, B. J.; Raja, S.; Yathindra, N. *Biophys. Chem.* **2002**, *95*, 253–272.
(41) (a) Prabhakaran, M.; Harvey, S. C. *Biopolymers* **1988**, *27*, 1239–1248. (b) Trieb, M.; Rauch, C.; Wibowo, F. R.; Wellenzohn, B.; Liedl, K. R. *Nucleic Acids Res.* **2004**, *32*, 4696–4703.
(42) Polak, M.; Manoharan, M.; Inamati, G. B.; Plavec, J. *Nucleic Acids Res.* **2003**, *31*, 2066–2076.
(43) Tian, Y.; Kayatta, M.; Shultis, K.; Gonzalez, A.; Mueller, L. J.; Hatcher, M. E. *J. Phys. Chem. B* **2008**, *113*, 2596–2603.

phosphate oxygens in the 2′,5′ RNA complex would provide a larger enthalpic contribution to binding than typical H-bonds.[44] Although proflavine has also been shown to form amine-phosphate oxygen H-bonds in complex with 3′,5′ RNA,[8b,f] the full enthalpy of these interactions may not be evident in the *net* enthalpy of proflavine binding. Apparently, in order for the 3′,5′ RNA backbone to participate in these H-bonds it must maintain all *North* sugar puckers around the intercalation site, and not the more energetically favored alternating *North*/*South* pattern of sugar puckers.[8d] In contrast, the intercalation-favored *South*/*North* pattern of sugar puckers for 2′,5′ RNA is compatible with the formation of these H-bonds in the 2′,5′ RNA−proflavine complex. The more favorable enthalpy of proflavine binding to 2′,5′ RNA may also reflect a greater difference in the enthalpy of stacking interactions between the intercalated and unintercalated states of 2′,5′ RNA, as compared to the two analogous states of 3′,5′ RNA.

Ethidium could presumably form H-bonds with the 2′,5′ RNA backbone similar to those of proflavine and also stack similarly with the bases, but thermodynamic measurements reveal almost no difference between the enthalpy of ethidium binding to both forms of RNA. It is possible that ethidium also participates in more favorable hydrogen bonding and base stacking with 2′,5′ RNA than 3′,5′ RNA but that these enthalpic gains are balanced by equally destabilizing interactions. For example, it was noted by Premraj et al. that the minor groove width of the 2′,5′ RNA helix is ∼1 Å less than that of 3′,5′ RNA.[40] This structural difference could severely disrupt the minor groove packing interactions observed for the phenyl and ethyl of intercalated ethidium in the 3′,5′ RNA crystal structure.[8e]

Acridine orange represented an opportunity to probe how the thermodynamics of binding would change if the H-bonds between proflavine and 2′,5′ RNA were disrupted. Consistent with this expectation, the favorable ΔH of proflavine binding to 2′,5′ RNA decreases from −11.0 to −5.3 kcal/mol when the exocyclic amines are methylated. It should be noted, however, that the binding free energy of acridine orange to 2′,5′ RNA might also be less favorable compared to proflavine because acridine orange has a self-association constant in water that is an order of magnitude higher than that of proflavine,[45] although little difference is observed between the thermodynamics of proflavine and acridine orange binding to 3′,5′ RNA.

Conclusions

We have shown that proflavine binds in the same orientation with the same nucleotide step preference as that observed for 3′,5′ nucleic acids. However, when proflavine intercalates 2′,5′ RNA there is a larger enthalpic gain compared to 3′,5′ RNA, which could be due to more favorable hydrogen bonding (charge−charge) and increased net stacking interactions in 2′,5′ RNA while maintaining most favored sugar puckers.

We have also identified several structural features that are common between proflavine intercalated 2′,5′ RNA and 3′,5′ RNA duplexes. These common features include the unwinding angle, change in helical rise, and the compact/extended sugar pucker motif at the intercalation site. Our results suggest that two structural transitions are coupled in the creation of an intercalation site; ζ rotates from the *-gauche* conformation to the *trans* conformation and the purine at the 2′ end of the binding site changes from a *South* (compact) to a *North* (extended) conformation. The data presented here are therefore consistent with the proposal of Kollman and co-workers in that the observed alternating sugar pucker is the most energetically favorable conformation,[8d] even with RNA containing different backbone connectivity.

As the single example presented here illustrates, ligand binding to nucleic acids with an alternative backbone provides fresh insights regarding the structural requirements for intercalation and the thermodynamics of ligand binding. Additional studies of ligand interactions with modified nucleic acids could further facilitate our understanding of the molecular recognition of natural nucleic acids. A more in-depth understanding of such interactions could also facilitate the development of molecular systems that allow protein-free template-directed synthesis (including prebiotic models)[46] and intercalation-driven nanostructures[47] that utilize Watson−Crick base pairs as well as noncanonical base pairs.[48] Finally, even the long-elusive origin of the nearest-neighbor exclusion principle appears obtainable through the use of modified nucleic acids.

Acknowledgment. We thank Profs. Janez Plavec, S. David Sherrill, Loren D. Williams, and W. David Wilson for helpful discussions. This work was supported by The National Science Foundation [Grant No. CHE-0404677], NASA Exobiology [Grant No. NNX08A014G], and The Georgia Cancer Coalition.

Supporting Information Available: Circular dichroism data, ^{1}H and ^{31}P NMR assignments for 2′,5′ RNA and proflavine, ζ angle analysis, and more in-depth thermodynamic analysis. This material is available free of charge via the Internet at http://pubs.acs.org.

JA810068E

(44) Rehm, T.; Schmuck, C. *Chem. Commun.* **2008**, 801–813.
(45) (a) Costantino, L.; Guarino, G.; Ortona, O.; Vitagliano, V. *J. Chem. Eng. Data* **1984**, *29*, 62–66. (b) Ortona, O.; Costantino, L.; Dellavolpe, C.; Vitagliano, V. *J. Mol. Liq.* **1990**, *45*, 201–211.
(46) (a) Hud, N. V.; Jain, S. S.; Li, X.; Lynn, D. G. *Chem. Biodiversity* **2007**, *4*, 768–783. (b) Jain, S. S.; Anet, F. A. L.; Stahle, C. J.; Hud, N. V. *Angew. Chem., Int. Ed.* **2004**, *43*, 2004–2008. (c) Hud, N. V.; Anet, F. A. L. *J. Theor. Biol.* **2000**, *205*, 543–562.
(47) Persil, Ö.; Hud, N. V. *Trends Biotechnol.* **2007**, *25*, 433–436.
(48) (a) Polak, M.; Hud, N. V. *Nucleic Acids Res.* **2002**, *30*, 983–992. (b) Jain, S. S.; Polak, M.; Hud, N. V. *Nucleic Acids Res.* **2003**, *31*, 4608–4615. (c) Persil, Ö.; Santai, C. T.; Jain, S. S.; Hud, N. V. *J. Am. Chem. Soc.* **2004**, *126*, 8644–8645. (d) Çetinkol, Ö. P.; Hud, N. V *Nucleic Acids Res.* **2009**, *37*, 611–621.